Application of Lock-In Thermography for Detecting Leakage Defects in Historic Masonry Arch Structures

Mohammed Fadhil Hama[1] & Ilham Ibrahim Mohammed[2]

[1&2]Faculty of Engineering, Department of Civil Engineering, Tishk International University
Sulaymaniyah, Iraq
Correspondence: Mohammed Fadhil Hama, Tishk International University, Sulaymaniyah, Iraq.
Email: mohammed.alzahawi@tiu.edu.iq

Abstract: Defects in masonry are difficult to detect with the naked eye. Non-destructive testing (NDT) techniques are one such ways to detect defects. One way to detect moisture is by using lock-in Infrared (IR) thermography technology. The main objective of this research is to detect a defect in masonry brick walls using infrared thermography camera. Infrared thermography tests were conducted in the laboratory on several experiments to understand time and temperature relationships. Tests were conducted on a masonry water tank with a known defect spot and were successfully detected from the thermography images. Two active approach methods were conducted: halogen lights and a heat gun. It has been shown that when using the heat-gun it is a quicker method according to the results. All procedures and methods performed in this report could be useful for field studies.

Keywords: Infrared Thermography, Non-destructive Defect Analysis, Masonry, Historic Structures, Defects, Image processing, Active Thermography

1. Introduction

The transportation system in Britain consumes over 40,000 masonry arch structures that compromise 40% of the road bridge stock and 33,000 railway arch spans. The British Transportation network boasts many masonries arch structures that make up an integral part of the nation's infrastructure. Although the construction of masonry bridges has long been abandoned in the UK, the bridges of the UK's network are still primarily masonry and brick with around 40,000 masonry highway bridges and. Many of these structures are 100 years old and are now subject to factors such as increased traffic loads and speeds that surpass the design requirements of that of over 100 years ago, causing some of them to incur damages or to gradually deteriorate (McKibbins, et al., 2006). Weathering of these masonry structures is a lead cause of deterioration of brickwork and structural issues can, a lot of the time, be traced back to water infiltration (Clark, et al., 2003). When a defect is present in a masonry arch bridge, the water infiltrates through the defect spot which normally spreads all over the area. For this reason, it makes it unable to detect where it is exactly leaking. An example of such defects is shown in figure 1 under a masonry arch bridge taking in Nottingham, UK. Suggestions made by deterioration rate studies have concluded that such structures deteriorate slowly between 50 years in its design life, which follows to a rapid deterioration during the last decade.

Even though that these are just prediction, if they are however correct, massive rehabilitation and reconstruction overheads are to be prepared over the next couple of decades (Anand, et al., 2003). To address such problems, it is a vital choice to consider actions taken as soon as possible. Such actions could be done using non-destructive testing (NDT) techniques to spot defects present in such structures. One of the new ways to detect moisture is by using Infrared (IR) thermography technology (Lagüela, et al., 2012). This paper will concentrate on the identification of moisture as an indicator of the point of defect of masonry arch bridges.

Figure 1: Defect in masonry arch bridge (The Arboretum, Nottingham)

2. Research Objectives

The objective of this research is to determine and verify whether the method of "lock-in thermography" is suitable to identify hidden defects in masonry arch structures. Two active approaches (i.e., hot air gun & halogen lights) will be used to determine and prove whether it is the suitable method or not. Also, this research will recommend which of the two active approaches is the more suitable method for the detection of defects in masonry arch structures.

3. Background Review

In terms of structural buildings, historical structures are very well cherished in many countries especially in the UK. It is vital to preserve such structures and to provide any necessity to keep the structure vigorous. This involves broad studies in maintaining them, by implicating scientists, architects, engineers, etc. Various historical structures undergo serious problems due to moisture content caused by weather conditions or by internal leakages in the structure itself. Such complications have impact on such historical structures or to a certain material of the structure (Castillo, et al., 2012) & (Bagavathiappan, et al., 2013). A correct verdict would be to eliminate such damaging effects caused by moisture content, nonetheless, to minimize the destructive effects. In other words, investigations are important aspects to collect data and outline any complication due to the conditions mentioned above. With such studies, many or all tackle could be eliminated and could also be used as maintenance purposes (Wild, 2007). For such cases, the use of non-destructive investigation techniques (NDT) is noteworthy for such indicative studies, particularly for in-situ surveys (Balaras & Argirou, 2002). NDT is a blameless solution for working out problems and to have investigations in historical buildings (Abdel-Qadera, et al., 2008). In such cases approaches of investigations allow the assessment of existing conditions of building materials without any damage to the existing building (Meola & Giorleo, 2004) & (Maldague, 2001). Many of the moisture defects are found on wall sections, which can have sub-layers that have different moisture content and defects caused by material failure and

cracks. Such types are expected to show different thermal inertia characteristics during heating or cooling down with external heating/cooling devices (Grinzato & Marinetti., 2002). To measure such characteristics precisely and practically, an infrared thermo-imaging camera (IR) can be used (Ostrowski, et al., 2003). The camera processes the surface temperature and the data for each image can be used to find the cooling/heating rate of the surface or a targeted area as a function of time. The temperature increases or decrease measured by the IR camera, with same climatic conditions, is due to different materials, or section of a structure, to either absorb or release heat (Meola, 2007). Different materials, depending on their porosity, can have different temperature changes with respect to time. In masonry structures one of the many defects is known as cracks, however, sometimes there could also be leakages in such walls due to poor workmanship in layering the bricks with mortar. Not sufficient mortar between each brick causes such leaks in structures, if suspected to water drainage. While cracks have large effect of structure stability, leaks may have little effect, although in a long period of time this could be a link cause to further damaging criteria's (Sowden, 1990). To examine such defaults, it is important to know which direction, amount, width, depth, and position of the defect(s). Another good achievement would be to determine the main reason of the defect. To determine in-situ defects should be preferable done by NDT methods, i.e. (IR thermography) (Grinzato & Marinetti., 2002).

A paper by (Pleşu, et al., 2012) gives a brief description of the theoretical background which states that IR thermography is a modern NDT for examining of renewed and non-refurbished structural buildings, where it offers a means for temperature measurement in structural buildings from the inside & outside of a building. It is also mentioned that the NDT has a main purpose to provide information by analysing the real characteristics of an existing structural building to determine surface irregularities such as cracks, voids, etc. Other authors (Meola & Giorleo, 2004) & (Maldague, 2001) have mentioned that NDT is a feasible solution to be used in historical and listed buildings, where the building cannot be damaged. In these kinds of investigations, the building should be assessed regarding its existing conditions and building materials.

When one of first IR thermography camera devices came into the industry, it had some perceived limitations in temperature climates that is too cold and where no or rarely solar exposure is available. However, with the advancement of current IR thermography devices available today it can detect smaller surface temperatures with changes of 0.01 °C (Grinzato & Marinetti., 2002) & (Kylili, et al., 2014).

Many efforts in research have been put into the use and development of IR thermography on different types of structures. The consequences from such research have led many companies to use these systems for indoor and outdoor structural surveys. It has been proven that IR thermography can detect problems such as voids (Meola, 2007), detached areas (Hola & Schabowicz, 2010), and deposits of humidity (Avdelidis, et al., 2003).

A paper by (Clark, et al., 2003) mentioned that although with the low ambient temperatures, there is a great potential to use IR thermography to detect and recognize areas, such as on a wall, that have defects such as delamination or other types of faults. The camera processes the surface temperature and the data for each image can be used to find the cooling/heating rate of the surface or a targeted area as a function of time (Theodorakeas, et al., 2014). The temperature increases or decrease is measured by the IR camera, under the same climatic conditions which can then be related to different materials, or section of a structure, to either absorb or release heat. Different materials, depending on their porosity, can have different temperature changes with respect to time (Balaras & Argirou, 2002)

& (Clark, et al., 2003). A paper by (Abdel-Qadera, et al., 2008) presents a project with the objective to program the detection of subsurface defects in concrete bridge decks using IR thermography. (Abdel-Qadera, et al., 2008) established an algorithm with the purpose that it is based on the region growing approach that segments the image and identifies the voids without human interference or previous awareness of the conditions. According to (Abdel-Qadera, et al., 2008) the results showed positive identified defects in the concrete bridge decks of defects up to 8 cm below the surface.

A paper by (Huang & Jer-WeiWu, 2010) describes "the multilayer level set method" to identify surface defects within a material. It is mentioned that the method depends on the inspection of temperature differences within the material. The test that was engaged to assess the performance of their algorithm; the artificial defectors are buried behind and near the surface of a structure covered with carbon fibre reinforced plastics. A set of halogen lights were used to heat the structure and images were taken.

An interesting paper by (Fox & Coley, 2014) presents a review of the existing literature covering both emerging and well-established building thermography methodologies. (Fox & Coley, 2014) claimed to have formed a clearer picture by critically appraising techniques and observing methodology applications for specific energy related defects. According to (Fox & Coley, 2014) the clearer picture helps thermography researchers and thermographers to decide upon the best methodology for performing building thermography investigations and for the invention of new approaches. Also, IR thermography is familiar as a non-destructive testing (NDT) by the ACI committee 228 (ACI , 1998) in section 2.7, being used in concrete construction for evaluation of the state of older concrete for rehabilitation purposes and quality assurance of concrete repairs.

3.1 Active and Passive Thermography

The IR thermography can be separated in two methods:

- Passive approach
- Active approach
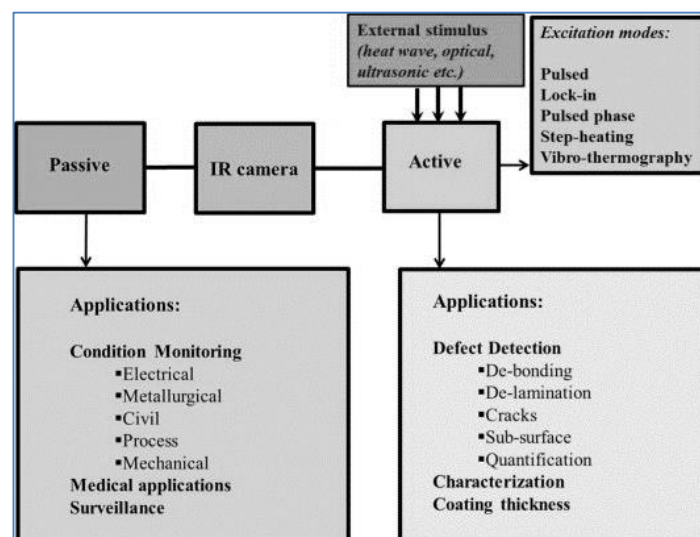
Figure 2: Active and Passive thermography (Bagavathiappan, et al., 2013)

Passive approach: In the applications mentioned for the passive approach, any unusual temperature profiles designate a potential problem to work on and to fix. The technique is established by using solar radiation, this is done to collect and record the thermal images without external system of heating or cooling applied to the object (Stimolo, 2003).

Active approach: This method is divergent to the passive approach. For this approach, an external heater or cooler is required to produce related temperature differences that are non-present otherwise. With the known features of the external stimulus, it gives the opportunity to have quantitative description (Poksinska, 2007).
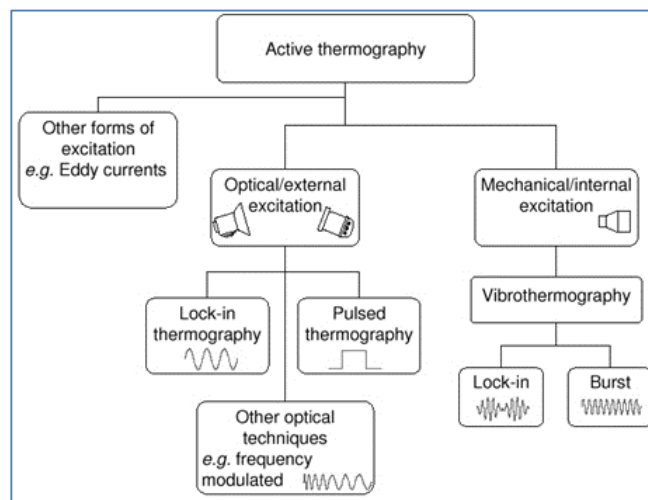
Figure 3: Active thermography (Maldague, 2007)

4. Methodology

The type of camera that was used was a FLIR-B 360 series. Figure 4 presents the steps taken to achieve the objectives.

1. Fundamental Parameters

2. Calibration at different position

3. Effect of Moisture by Relating Time and Temperature

4. Active Thermography of Masonry "water tank"
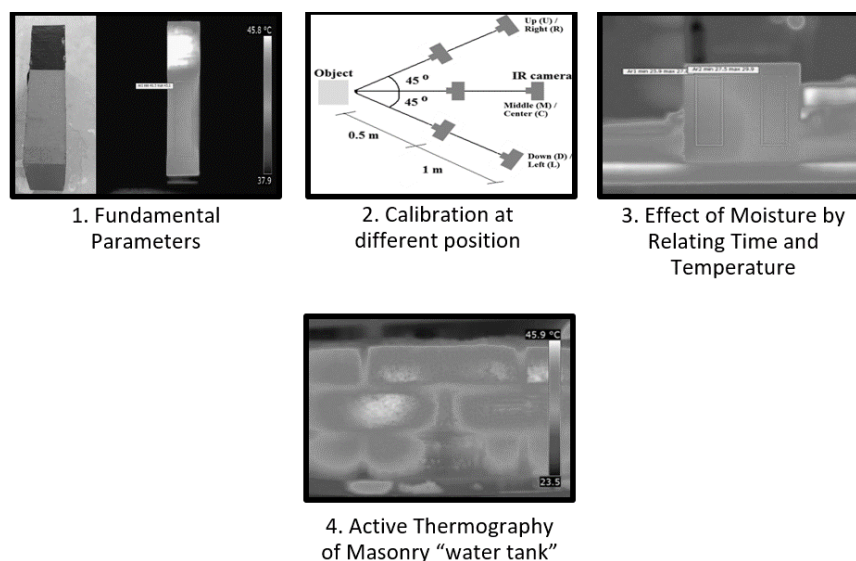
Figure 4: Methodology process

4.1 Fundamental Parameters

The IR thermography camera processes and captures the emitted infrared radiation from a material or any object. The IR thermography camera can calculate and show the temperature of an object since its radiation is a function of the objects surface temperature. However, the measured radiation by the IR thermography camera is not only dependent on the temperature of the material or object; it is also a function of the emissivity. The reflected radiation and the radiation from the materials or objects are also subjective by the absorption of the atmosphere. Several different effects of different radiation sources are required to be recompensed to have and accurate temperature measurement. With the easy technology available today, all this can be done "on-line" automatically by the camera. However, some object parameters must be provided for the IR thermography camera:

- The atmospheric temperature
- The relative humidity
- The reflected apparent temperature (This parameter is used to recompense for the radiation reflected in the object. The reflected temperature has been found using the FLIR B-series manual known as "Reflector method".)
- The distance between the object and the camera
- The emissivity of the object (This method has been explained in the FLIR B-series manual as shown in figure 5.)

1	Select a place to put the sample.
2	Determine and set reflected apparent temperature according to the previous procedure.
3	Put a piece of electrical tape with known high emissivity on the sample.
4	Heat the sample at least 20 K above room temperature. Heating must be reasonably even.
5	Focus and auto-adjust the camera, and freeze the image.
6	Adjust **Level** and **Span** for best image brightness and contrast.
7	Set emissivity to that of the tape (usually 0.97).
8	Measure the temperature of the tape using one of the following measurement functions: ■ **Isotherm** (helps you to determine both the temperature and how evenly you have heated the sample) ■ **Spot** (simpler) ■ **Box Avg** (good for surfaces with varying emissivity).
9	Write down the temperature.
10	Move your measurement function to the sample surface.
11	Change the emissivity setting until you read the same temperature as your previous measurement.
12	Write down the emissivity.

Figure 5: Finding emissivity of object (FLIR B-series manual) Thermography images at different positions (Calibration)

In practical life (in-situ), taking thermo images by an IR thermography camera cannot always be taken at any place desired. For example, taking images under a bridge in which beneath a river flows, the

person must stand beside the bridge at an angle to capture the necessary images. An example of such case is illustrated in Figure 6.

Figure 6: Inaccessible Masonry Bridge from beneath (Glasgow, UK)

For this instance, an evaluation has been carried out in the laboratory to understand if the same surface temperature indicated from the IR thermography camera changes of a particular object at different positions. Figure 7 illustrates where the different images has been taken. To evaluate the surface temperature obtained from the IR thermography camera, the images were captured at different angles and distances away from the object.
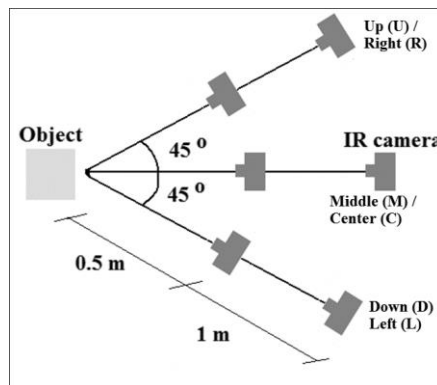
Figure 7: Top and Side view of images captured by IR camera (18 images) Time and temperature relationship.

To evaluate the time and temperature relationship, the active approach using the lock in thermography has been done on cement cubes. Four cement cubes sizes of 10 x 10 x 10 cm have been used in the assessment. All four cubes were kept for 24 hours in a buckle of water. The water level in the bucket was kept a little lower than half the height of the cubes. This was done to have half of the cube to be fully in moisture and the other half (fully) dry. Three of the four cubes were kept in room temperature and one of them was kept in cold water and in a cooler to have a colder temperature. Figure 8 illustrates how the cubes were kept in the bucket.
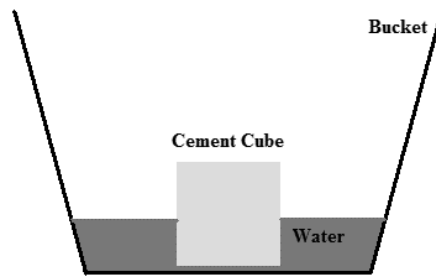
Figure 8: Cement cube in bucket

Each cube was then taken and assessed using the IR thermo imaging camera. The cubes were investigated in the laboratory under its environmental conditions. The cubes were externally heated up with two halogen lights with each having 500 watts at 0.5 m as illustrated in in figure 9. The IR thermography camera was kept at 0.7 m.
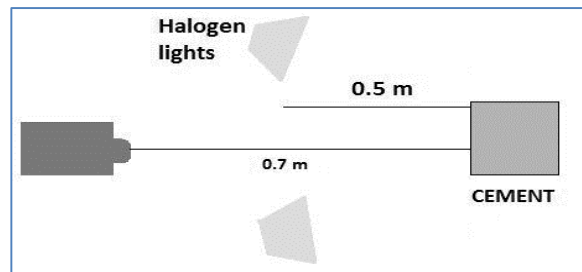
Figure 9: Cement cube tested

When the images are to be captured, the initial pictured is to be expected that the "wet" side has the same average temperature as the "dry" measured with the QuickReport software from the images captured. To have a good evaluation, an image will be captured using the IR thermography camera every minute manually. The taking of images will be manually done since the available camera (FLIR B-360 series) does not have a video recording option. The time will be observed using a stopwatch. All four cubes are to be investigated with the procedure to have two parameters: time vs. temperature. However, it is to be noticed that the type of heat source, the distance between the heat source and the object and the environmental conditions in the surrounding area influence the results.

4.2 Active Thermography of Masonry "Water Tank"

Many masonry walls have leaking's due to cracks in the brick or in the mortar between the bricks. Also, leaks could be caused by poor workmanship at the time it was constructed; by not keeping enough mortar between the bricks causes the water to infiltrate through the mortar and cause leaks. Such leaks cannot be easily found with the naked eye. However, a wall which is moisturized has a lower temperature than the dry side. Although, when a defect is present, the water that infiltrated through the defect normally spreads all over the area, which makes it unable to detect where it is exactly leaking. Figure 1 clearly shows the wet area and the dry area. Nevertheless, it is unable to detect the defect with the naked eye. For this reason, a masonry water tank has been constructed in the laboratory with a known defect. The masonry water tank is illustrated with the indicated defect in Figures 10 & 11.
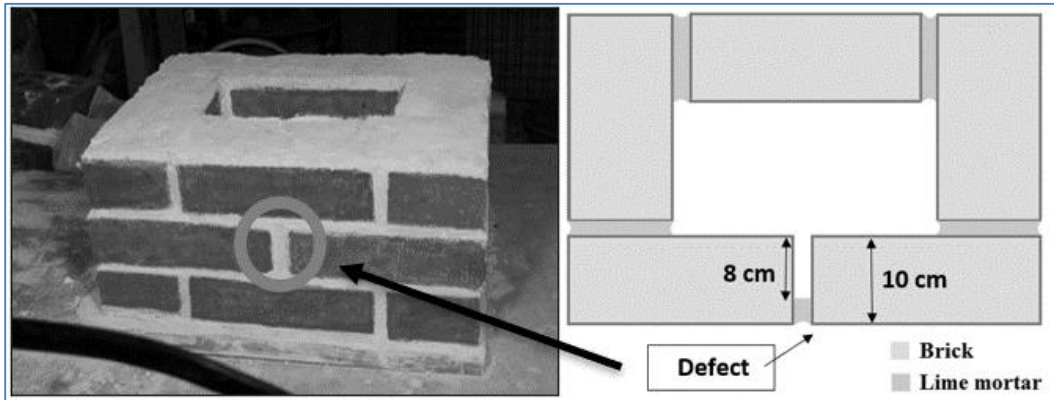
Figure 10: Masonry water tank

The tank is built in such a way so that the water can easily infiltrate through the 2 cm thick defect. All measurements and parameters of this report are to be considered and corroborated. To apply the lock in thermography method, two approaches will be done on the masonry water tank to excite the surface temperature with heat to dry up the surface:

- Halogen lights with each of 500 watts at distance of 0.5 metre
- Hot air gun, heating up the whole surface to make the surface fully dry.

However, the question may be raised that there are two different materials used in the procedure, and which emissivity value to use. Since both materials have close emissivity value close to each other, 0.78 (lime) and 0.75 (brick), according to (Barreira & Freitas, 2005) this does not matter much since the temperature does not make a difference when the emissivity value is changed from 0.78 to 0.75.

Both active approached are to be prepared as follows:

4.2.1 Halogen Lights with Each of 500 Watts at Distance Of 0.5 Metre

In this method, two halogen lights with each having 500 watts of power will be set 0.5 metres away from the masonry water tank and the IR camera will be put 0.8 metres away from the masonry water tank. The procedure will be done in a way that an image is captured every minute until a picture will show justifiable results to be able to trace the defect by a qualitative way. The arrangement has been show in Figure 11.
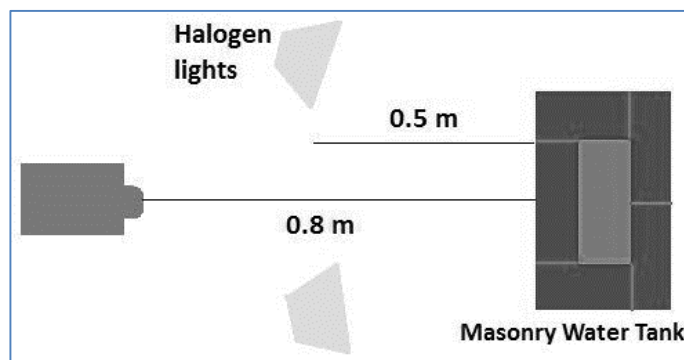
Figure 11: Halogen lights method set-up

4.2.2 Hot Air Gun, Heating up the Whole Surface to Make Surface Full Dry

In this method, an ordinary hot air gun (Figure 12) will be used to heat up the surface to get the full surface dry. Since the device has a small diameter for the air flow coming out of the gun, the user must come close to the surface (3 ~ 5 cm distance). The speed to heat up the surface is recommended to be 2 cm/second, this ensure the surface to be fully dry without causing any damage to the device itself or maybe the wall. However, it is recommended to heat the brick area first then the joints between the brick. Heating the bricks takes less time and dries up quicker than the lime. The assessment will be done somewhat different then the first method with the halogen lights. In this case the tank is first fully wet for 24 hours room temperature water. The hot air gun is then applied over the whole surface for approximately 4 minutes making the whole surface fully dry. At last, the tank is let to be cooled down. For each of these three phases an image will be captured with the IR thermography camera. In each image a line segment will be on the vertical joints between the bricks. The lines segments are then transformed to an excel spread sheet and plot into graph to differentiate between time and temperature in three phases: i.e. wet, heating, cooling.

Figure 12: Air Gun

5. Results

5.1 Fundamental Parameters

For fundamental parameters, all requirements according to the FLIR B-series manual were carried out and evaluated in the laboratory. Each step was taken specifically as mentioned in the manual. All the five parameters have been carried out in the laboratory to provide the inputs for the IR thermography camera FLIR B-360 and the results obtained are explained next:

The atmospheric temperature:

This temperature is the temperature between the IR thermography camera and the target. The atmospheric temperature was 24 °C of the laboratory where all tests and investigations were taken place using a thermostat available from the laboratory.

The relative humidity:

According to the manual of the FLIR B-series, for short distances and normal humidity, such as in laboratories or at indoor, the relative humidity can normally be chosen at a default value of 50%.

The reflected apparent temperature:

From the thermo image captured (Figure 13), the procedure is done by using the FLIR QuickReport software included with the camera. The reflected apparent temperature has been found to be 28.5 °C.
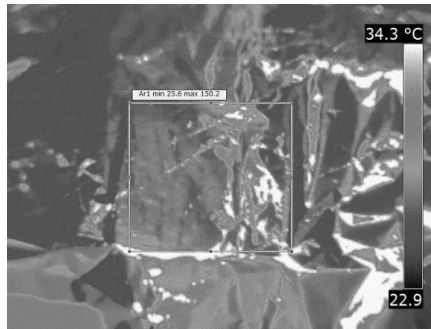
Figure 13: Thermo image of aluminium foil

The distance between the object and the camera:

The distance set is the distance between the object and the front lens of the camera. This parameter is for the following two specifics:

- The radiation from the target is absorbed by the atmosphere between the material or object and the camera lens.
- The radiation from the atmosphere itself is detected by the camera.

The distance was measured using a normal measuring tape.

The emissivity of the object:

This procedure has been carried out for three materials: cement, lime, and masonry brick.
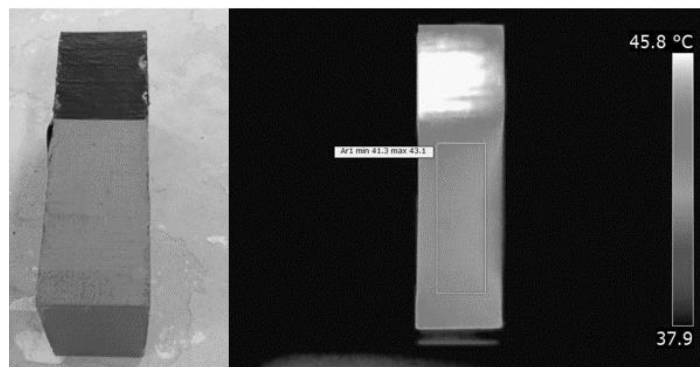
Figure 14: Prepared sample with black tape (left), Captured image of masonry brick to find its emissivity using FLIR QuickReport (right)

All three samples have been heated up at least 20 °C above room temperature using to halogen lights of 500 watts each. The following table shows the emissivity values obtained from the laboratory assessment:

Table 1: Emissivity values found

Material	Emissivity (ε)
Lime	0.78
Cement	0.85
Masonry brick	0.75

5.2 Thermography Images at Different Positions (Calibration)

A total of 18 images were captured and assessed using QuickReport software to find the average temperature of the object's area at different positions. Figure 15 shows all the images captured, and Table 2 shows the average surface temperature for each image captured.
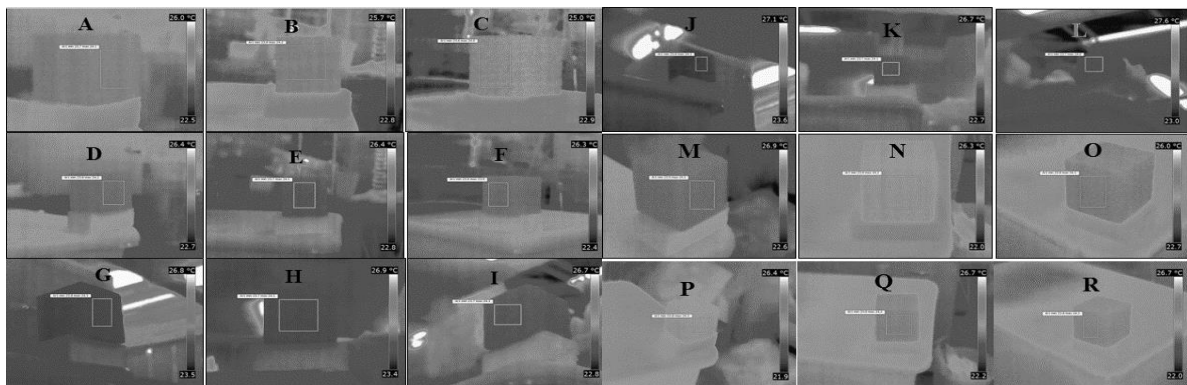
Figure 15: Images captured from different positions and angles

Table 2: Average temperature of each thermo-image

	Average surface temperature (°C)
Minimum =	23.8
Maximum =	24.1
Average =	23.9

The object was set to room temperature and no external heating/cooling was applied to the object to have a linear surface temperature of the object. The total of 18 image's surface temperature, in table 2, show that the minimum temperature to be 23.8 °C, maximum of 24.1 °C, and the average of the total images to be 23.9 °C. This indicates the difference in temperature only showed a difference between the images to be ±0.3 °C. Although these images were taken of the same object and same surface, it did show a small difference. It should be noted that when taking images from different positions, the surface visibility of the same area becomes different, change in shape and size. This makes a disadvantage when using the software QuickReport, since in the software only rectangles, points and lines can be chosen to identify the temperature of the pixels on or in the shape. In some of the images taken, the rectangles are different in shape; this might affect the average surface temperature of the chosen surface. Although it is the same object, some smaller areas might be affected by the environment, or these small areas can have slightly different texture that affects the emissivity value of the object.

5.3 Effect of Moisture by Relating Time and Temperature

In Figure 16, one of the cubes at initial time = 0 min has been illustrated with another image with t = 20 min and a final time when both surfaces reached almost fully dry.

(a) @ t = 0 min   (b) @ t = 20 min   (c) @ t = 81 min
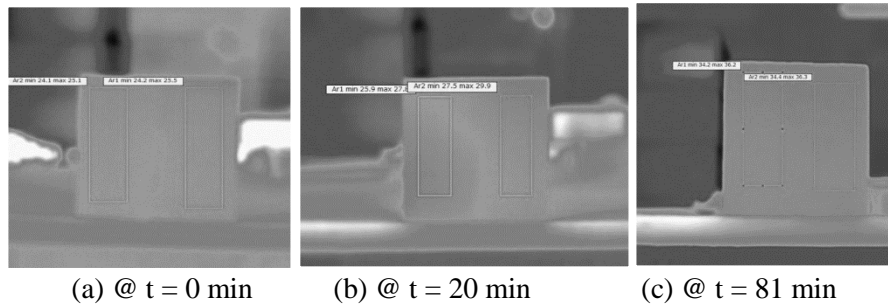
Figure 16: Cube tested

The results were obtained from all the images and assessed using the QuickReport to obtain the average area temperature of the "wet" side of the cubes (left side) and the average area temperature of the "dry" side of the cubes (right side). Each temperature was taken with its time captured and set in excel spread sheets. For each cube two graphs were plotted. One graph indicates the temperature curves of each side and the other to differentiate between the dry side and the wet side. The data was then plotted into graphs as seen Figures 17 - 20.
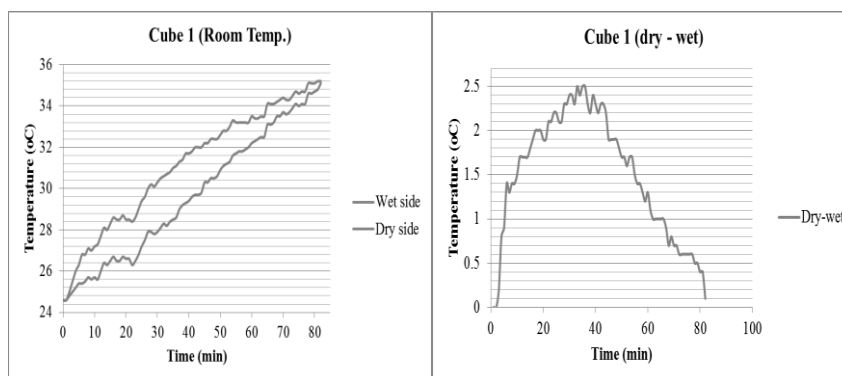
Figure 17: Cube 1 at room temperature
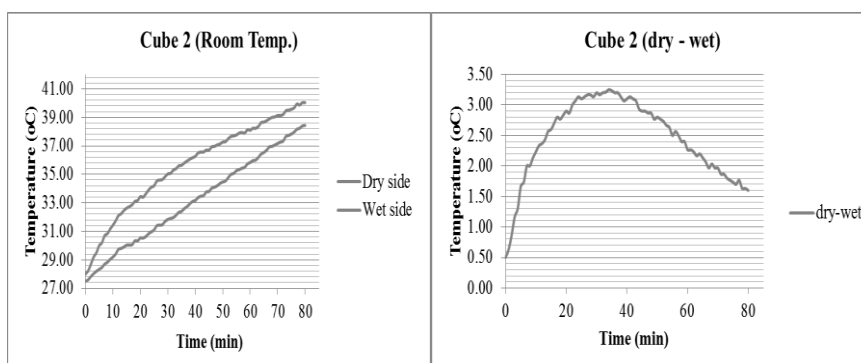
Figure 18: Cube 2 at room temperature
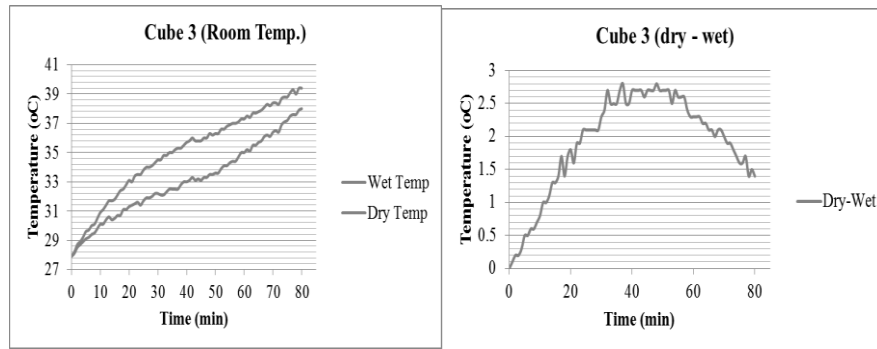
Figure 19: Cube 3 at room temperature
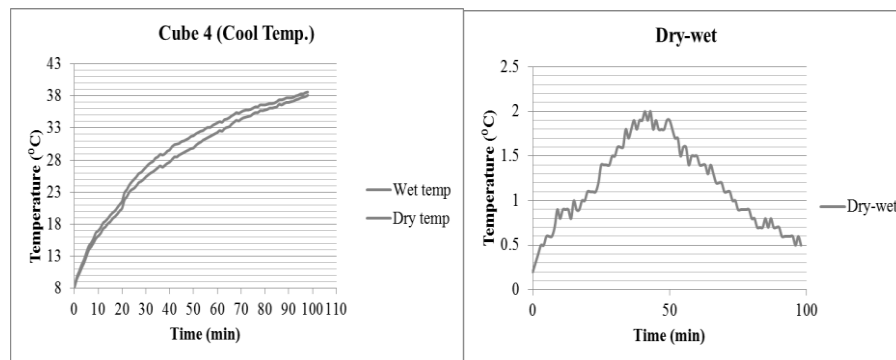
Figure 20: Cube 4 at cooler temperature

Table 3: Time to have maximum temperature difference between dry and wet side

Cube	Time (min.)
1	35
2	37
3	36
4	34

5.3.1 Analysis: Effect of Moisture by Relating Time and Temperature

All investigated cubes resulted to have the maximum temperature difference (between dry area and wet area) at around 35 minutes after heating up the surface (Table 3). This result is an indication to know how long the inspection investigation would take. However, it is essential to know that this investigation is limited. The limitations are that the heat source to be used must be two halogen lights with each having a power of 500 watts, kept at 0.5 m distance and only for cement material. The resulting time for this investigation may not imply on every material or if using higher or lower heat sources. However, the steps taken, and the analytical approach could be applied for any desired object with a different heat source and a different distance between the heat source and object to get the required time needed in order to differentiate between dry areas and wet areas. When the maximum temperature difference is known at its time, the inspector could then indicate the leak source on the structure.

5.4 Active Thermography of Masonry "Water Tank"

The water tank was then led to leak for 24 hours where water was kept introduced to the tank. Also, to make it more realistic, a wet towel which was made wet with the same water temperature, was kept over the surface of the tank to have the whole surface wet. This was done to make the surface temperature to one temperature. To validate this, an image was taken the next day and showed this to be correct as seen in Figure 21.

Figure 21: Masonry water tank with average surface temperature of 22.4 °C

To ensure which emissivity value has to be taken since there are two different materials, with the aid of the software QuickReport, when choosing the same area as seen in in figure 21, the emissivity values have each been inserted and showed that the difference in temperature is only ± 0.1 °C. However, in this case the emissivity value of 0.78 (lime) is chosen since the lime is the critical part of the suspected defect. Both active approaches have been assessed and resulted as follows.

5.4.1 Halogen Lights with Each of 500 Watts at Distance of 0.5 Metre

The first captured image (at 1 minute after putting the lights on) and the last captured image are shown in Figure 22. The figures show that by heating up the surface it clears up much of the moisturized surface area.
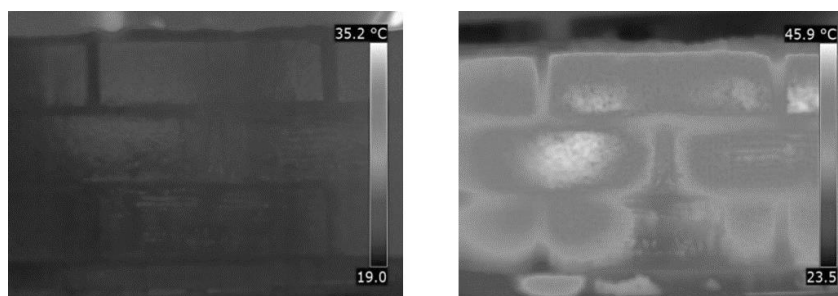
(a) @ time = 1 minute of heating   (b) @ time = 30 minutes of heating

Figure 22: Difference of surface temperature after heating

The areas that had no defect clearly showed that it dried up, speaking in a qualitative manner. However, to evaluate it in a quantitative manner, line segments using the software QuickReport have been put over the vertical joints between the brick to differentiate between the 5 joints. This has been done in the same images from Figure 22. These lines in the images are presented in Figure 23.
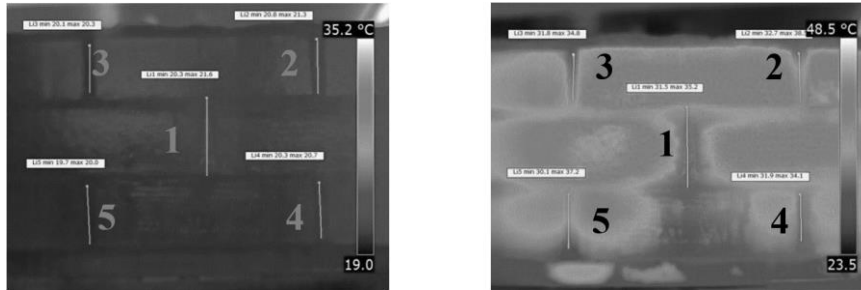
Figure 24: Indicating line segments.

Each of these lines indicated the temperature for each pixel along the line. These data have been transformed into excel spread sheets and presented in graphs. Figures 25 and 26 show these results.
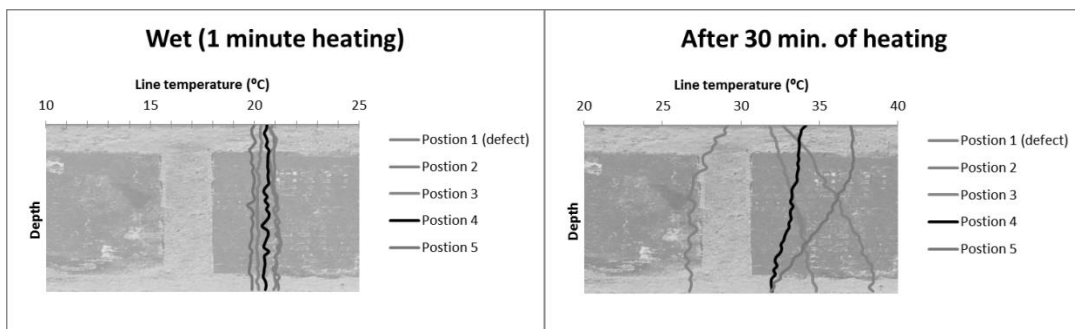
Figure 25: Line segments when heated with lights
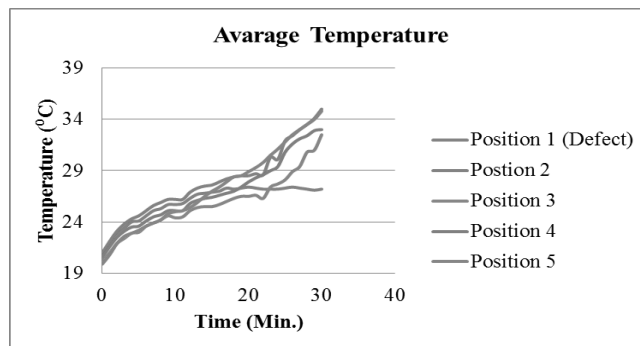
Figure 26: Average temperatures at every minute

5.4.2 Hot Air Gun, Heating Up the Whole Surface to Make Surface Fully Dry

In Figure 27 the images are being shown of all the three phases.

(a) Fully wet (t = 0 min)   (b) After heating (t = 4 min)   (c) Cooling (t = 10 min)

Figure 27: Three phases using hot air gun
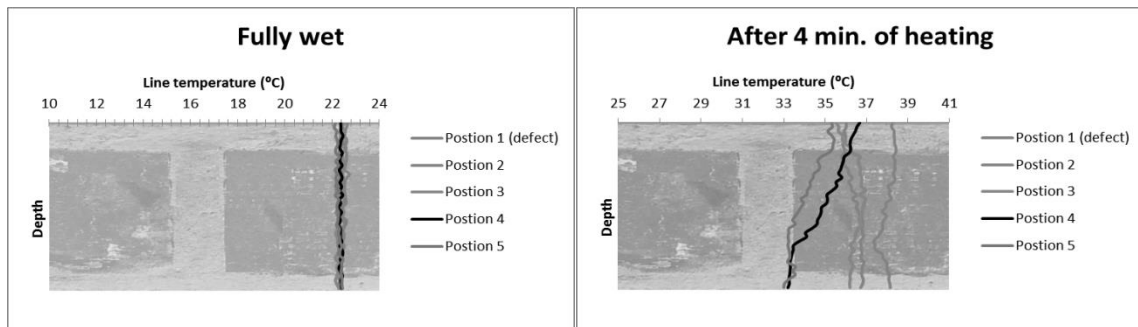
Figure 28: @ t = 0 min (left) and t = 4 min. (right)
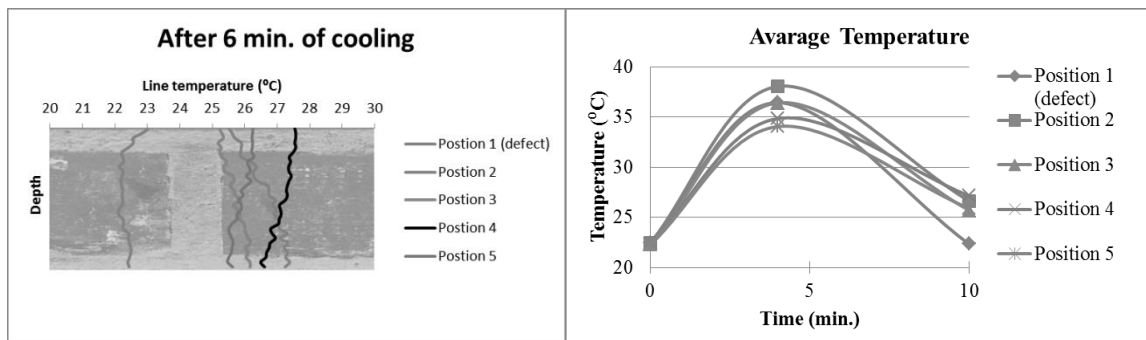
Figure 29: After cooling @ t = 10 min (left), Average temperatures at every minute (right)

However, to evaluate the process of using a hot air gun for detecting masonry defects further, instead of room temperature water, cold water was introduced in the masonry water tank to see if there would be any significant difference in the results other than having the temperatures lower. The procedure was carried out the same as the previous procedure and the results are shown in the following figures.
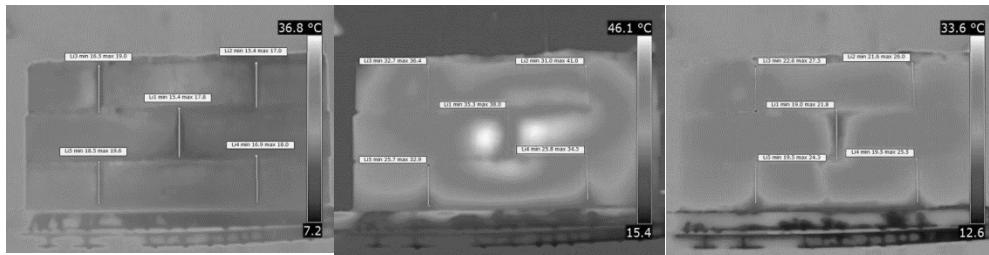
(a) Fully wet (t = 0 min)   (b) After heating (t = 4 min) (c) Cooling (t = 10 min)

Figure 30: Three phases using hot air gun (Cool water)
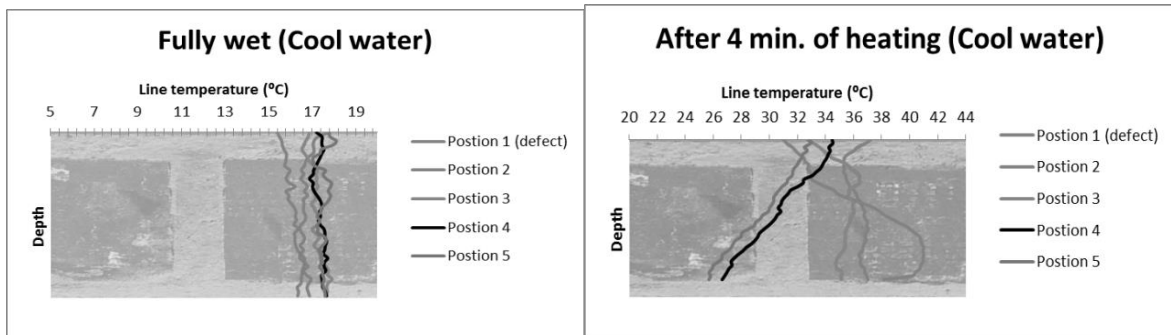
Figure 31: Line segments @ t = 0 (Cool water) (left) and @ t = 4 min (Cool water) (right)
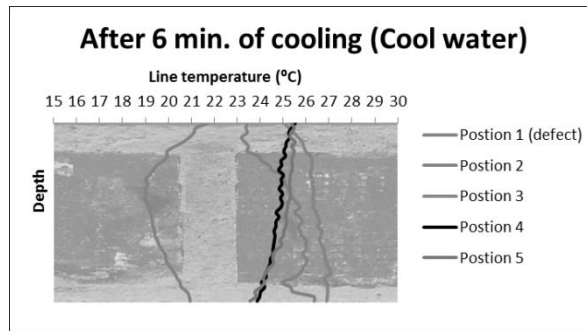
Figure 32: After cooling line segments at t = 10 min (Cool water)
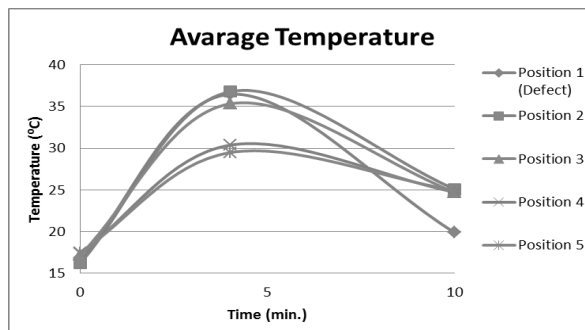
Figure 33: Average temperatures at every minute (Cool water)

5.4.3 Analysis: Active Thermography of Masonry "Water Tank"

The tank was constructed in such a way that the first leak should appear in the known vertical defect spot at the joint between the bricks. In Figure 24 this was demonstrated to be operational as expected. Although it is indicated that it started to leak after 5 minutes, this is however, not part of the analytical approach. It was proven when the emissivity value of 0.78 and 0.75 each were used as inputs in the QuickReport software to have almost the same surface temperature with a difference of ±0.1 °C.

For the first active approach, the halogen lights were used as a heat source to dry up the surface. From Figures 24 & 25 it can be seen, in a qualitative analysis, that after 30 minutes of heating up the surface, it noticeably showed where the defect is present. However, in this case the way the masonry tank was constructed, the moisturized part in the lime mortar did stay in the horizontal high upper and lower part of the tank. Discoursing in a quantitative way it has been clearly shown in figure 25 (left), that at all vertical joints are almost the same temperature at initial as expected. After heating up the surface for 30 minutes, in figure 25 (right), it has been visibly shown that the line of position 1 had the lowest temperature, which indicates the defect point. This is due that the water behind the heated-up surface is still at its original temperature, and when still leaking through the defect area, the moisture will not heat up as quickly as the un-defected areas by the heat of the light source. Also, Figure 26 clearly shows that position 1 is the defect spot at a certain time versus temperature.

In the second active approach using the hot air gun, almost the same first steps were taken when using the halogen lights. However, in this technique three images have been taken to differentiate and get accurate results. From figure 27 (a), its vertical line temperature results are presented in figure 28 (left). It can be undoubtedly seen that at all positions the temperatures were similar at initial (before heating) in figure 27 (a). The surface was then dried up (figure 27 (b)) using the hot air gun within just 4 minutes, and the results at each position has been plotted in figure 28 (right) which gave a disturbing difference in temperature at each position from 33 – 38 °C. However, just after 6 minutes of cooling, it showed very explicit results in figure 29 (left). The defect position 1 was very well noticed from the results. Also, differentiating between the images in the three different phases of figure 27, it is very well shown, in a qualitative approach where the defect point is after cooling down in just 10 minutes. Figure 29 (right) showed a clear view of the time and temperature relationship as expected and showed clearly that the defect spot is to be found at position 1.

The same approach was then re-evaluated with cooler water. It was expected to take a longer time to do the same three phases; however, it took the exact same time to get good results to detect the defect point as seen in the figures 30 – 33. Comparing the two active approaches, it can be certainly known that using the hot air gun is a much faster technique for detecting the defect position in this case. The second technique is done 20 minutes quicker than the first technique.

6. Conclusions

Based on the number of tests implemented in the laboratory, it is to be concluded that lock-in thermography can be used as an effective way for detecting defects in masonry brick walls. The following conclusions are drawn based on the laboratory experiments:

- It is found that when taking thermography pictures at different distances and angles to an object the temperature only makes ±0.3 °C difference. This concludes that taking pictures from different places would not matter for the interpretation and/or analysis part of the investigation.

- From the time and temperature relating graphs it shows that it takes around 35 minutes to have a maximum temperature difference between the wet and dry surfaces on the same object when using halogen lights sources. The halogen lights were each of 500 watts and kept at 0.5m from the object (concrete cube). With the given procedure in this research, it is recommended to use the same procedure for any other material and heat source to obtain the necessary time needed to do an active approach. The engineer could then know how much time is needed to do the procedure at pre-construction.

- Finally, the defect spot in the masonry water tank was easily located when using both active approaches. However, when using the hot airgun, the defect was spotted quicker and seen more clearly in the thermography image. It is to be noted when using the hot air gun, it is recommended to do it on a small area, and while using the halogen light sources, depending on the number of bulbs; it could be done on larger areas.

References

Abdel-Qadera, I., Yohalia, S., Abudayyehb, O., & Yehia, S. (2008). Segmentation of thermal images for non-destructive evaluation of bridge decks. *NDT&E International*, 41(1), 395-405.

ACI, 1998. Nondestructive Test Methods for Evaluation of Concrete in Structures ACI 228, Farmington Hills, MI, USA: ACI Committee.

Anand, K., Vasudevan, V., & Ramamurthy, K. (2003). Water permeability assessment of alternative masonry systems. *Building and Environment*, 1(38), 947 – 957.

Avdelidis, N., Moropoulou, A., & Theoulakis, P. (2003). Detection of water deposits and movement in porous materials by infrared imaging. *Infrared Physics & Technology*, 1, 183-190.

Bagavathiappan, S., Lahiri, B., Saravanan, T. & Philip, J., 2013. Infrared thermography for condition monitoring – A review. *Infrared Physics & Technology,* 60(1), 33-35.

Balaras, C. A. & Argirou, A. A., 2002. Infrared thermography for building diagnostics. *Science B. V.*, 34(4), 171-183.

Castillo, R. V. (2012). Thermal imaging as a non-destructive testing implemented in heritage conservation. *Journal of Geography and Geology*, 4(4), 102-113.

Clark, M., McCann, D., & Forde, M. (2003). Application of infrared thermography to the non-destructive testing of concrete and masonry bridges. *NDT&E International*, 36(2), 265-275.

Fox, M., & Coley, D. (2014). Thermography methodologies for detecting energy related building defects. *Renewable and Sustainable Energy Reviews*, 1, 296-310.

Grinzato, E. P. G. B., & Marinetti., S. (2002). Monitoring of ancient buildings by the thermal method. *Journal of Cultural Heritage*, 3, 21-29.

Hola, J., & Schabowicz, K. (2010). State-of-the-art non-destructive methods for diagnostic testing of building structures – anticipated development trends. *Archives of Civil and Mechanical Engineering*, 3, 20-39.

Huang, Y., & Jer-Wei, W. (2010). Infrared thermal image segmentations employing the multilayer level set method for non-destructive evaluation of layered structures. *NDT&E International*, 43(1), 34-44.

Kylili, A., Fokaides, P. A., Christou, P., & Kalogirou, S. A. (2014). Infrared thermography (IRT) applications for building diagnostics: A Review. *Applied Energy*, 1, 531-549.

Lagüela, S., Solla, M., Armesto, J., & González-Jorge, H. (2012). Comparison of infrared thermography with ground-penetrating radar for the non-destructive evaluation of historic masonry bridges. Vigo, Spain: Quantitative InfraRed Thermography.

Maldague, P. (2001). *Theory and practice of infrared technology for non-destructive testing*. New York: John Wiley & Sons.

Maldague, X. (2007). MIVIM. [Online] Retrieved on March 8, 2021 from http://mivim.gel.ulaval.ca/dynamique/index.php?idD=67&Lang=1

McKibbins, L. D., Melbourne, C., Sawar, N. & Gaillard, C. S. (2006). *Masonry arch bridges: condition appraisal and remedial treatment*. London: Classic House`.

Meola, C. (2007). A new approach for estimation of defects detection with infrared thermography. *Materials Letters*, 61(2), 747-750.

Meola, C. G. C., & Giorleo, L. (2004). The use of infrared thermography for materials characterization. *Journal of Materials Processing Technology*, 155-156, 1132-1137.

Ostrowski, C., Antczak, E., Defer, D., & Duthoit, B. (2003). Association of infra-red thermography and thermal impedance applied to the detection of empty spaces under concrete slabs. Béthune cedex, France: Non-Destructive Testing in Civil Engineering.

Pleşu, R., & Teodoriu, G. (2012). Infrared thermography applications for building investigation. Iaşi: Buletinul Institutului Politehnic Din Iasi.

Poksinska, W. B. (2007). Passive and active thermography application for architectural monuments, Padova, Italy: Proc. in the 8th Conf. on Quantitative Infrared Thermography.

Sowden, A. (1990). *The maintenance of brick and stone masonry structures*. London: CRC Press.

Stimolo, M. (2003). Passive infrared thermography as inspection and observation tool in bridge and road construction, Berlin, Germany: Proceeding in the International Symposium. (NDT-CE 2003).

Theodorakeas, P., Avdelidis, N. P., Cheilakou, E. & Koui, M. (2014). Quantitative analysis of plastered mosaics by means of active infrared thermography. *Construction and Building Materials*, 1, 417-425.

Wild, W. (2007). Application of infrared thermography in civil engineering. *Proc. Estonian Acad. Sci. Eng.*, 4(1), 436-444.